Electron transport in argon in crossed electric and magnetic fields

Kevin Ness
School of Computer Science, Mathematics, and Physics, James Cook University, Townsville, Queensland, 4811 Australia

Toshiaki Makabe
Department of Electronics, Keio University, 3-14-1 Hiyoshi, Yokohama 223, Japan

(Received 13 December 1999)

An investigation of electron transport in argon in the presence of crossed electric and magnetic fields is carried out over a wide range of values of electric and magnetic field strengths. Values of mean energy, ionization rate, drift velocity, and diffusion tensor are reported here. Two unexpected phenomena arise; for certain values of electric and magnetic field we find regions where the swarm mean energy decreases with increasing electric fields for a fixed magnetic field and regions where swarm mean energy increases with increasing magnetic field for a fixed electric field.

PACS number(s): 51.50.+v, 52.25.Fi, 51.10.+y

I. INTRODUCTION

In 1993 Ness [1] presented a general formalism for solving the Boltzmann equation for reacting charged-particle swarms in neutral gases in the presence of an electric and magnetic field set at some arbitrary angle to each other. The formalism used was based on a spherical-harmonic expansion in velocity space of the charged particle phase space distribution function. In a subsequent paper Ness [2] effected numerical solution of the Boltzmann equation for electron swarms by further expanding the energy dependence in terms of Sonine polynomials. This numerical solution was done for the geometry of perpendicular fields and conservation interactions between the electrons and neural molecules. In the present paper we extend the numerical solution to include ionization by electron impact, a nontrivial extension of the code (see next section). This work was motivated by research being carried out at the Department of Electronics, Keio University into the use of magnetron discharges for material sputtering, where argon is the primary gas used. For the remainder of the section a brief summary of the connection between swarm physics and the use of magnetron discharges in plasma processing will be given.

In the context of plasma processing a magnetron is a device that makes use of electric and magnetic fields to control and maintain the plasma under a lower pressure condition than is possible with an electric field only. The application of the magnetic field to a discharge under the influence of an applied electric field corresponds qualitatively to an increase in the neutral (argon) density. This effective or apparent increase in the neutral density is due to an increase of the residence time of the electrons in the plasma, brought about by the Lamor gyrations [3]. As a result we can expect a lower energy and a higher density of electrons at a lower pressure in a plasma when an external magnetic field is applied to the discharge [4]. Furthermore, since the Lamor radius of the ions is large compared to the dimensions of the discharge, the addition of the magnetic field will have negligible effect upon the ion transport. In this system the collision rate of the electrons with the neutrals can be controlled independently of the gas pressure by varying the strength of the applied magnetic field. This means that in a lower pressure magnetron plasma the ions from the sheath to the target will be essentially collisionless with a beamlike energy.

Magnetrons are used primarily for the process of sputtering in which energetic particles, such as ions, are used to eject material from a solid surface [5]. In the process of sputtering secondary electrons are produced. These secondary electrons are accelerated back through the plasma where they cause ionization of the neutral atoms and thus produce more plasma. In the plasma bulk, where the secondary electrons do most of their ionization the electric and magnetic fields are predominately perpendicular or near perpendicular. Since electrons are essential to maintain the plasma, a knowledge of their behavior, i.e., their transport coefficients, is important in the design and optimization of such devices [4]. These transport coefficients can be either measured in swarm experiments or calculated from transport theory. To date, no experiments exist that can measure all the required transport coefficients (rate coefficient, drift velocities, and diffusion coefficients) for electrons in gases in the present of electric and magnetic fields. In the present work we solve the Boltzmann equation for electron swarms undergoing ionization in argon in the presence of perpendicular electric and magnetic fields. In this application ionization by electron impact plays a key role in the electron behavior, therefore any modeling must treat ionization in a comprehensive manner.

II. THEORY

The theoretical approach used in the present work to solve the nonconservative Boltzmann equation can be found in Ref. [1] and [2]. For the sake of completeness a summary is presented here.

The starting point of the present analysis is the Boltzmann equation

$$\left[\frac{\partial}{\partial t}+\mathbf{c}\cdot\frac{\partial}{\partial \mathbf{r}}+\frac{e}{m}(\mathbf{E}+\mathbf{c}\times\mathbf{B})\cdot\frac{\partial}{d\mathbf{c}}+J\right]f(\mathbf{r},\mathbf{c},t)=0, \quad (1)$$

where e is the charge on, and m is the mass of an electron moving under the influence of an electric field of strength $\mathbf{E}$

and a perpendicular magnetic field of flux density **B**. The collision operator J takes into account the effect of binary collisions between the electrons and the neutral molecules on the electron motion. Formally Eq. (1) is solved for the single-particle phase-space distribution $f(\mathbf{r},\mathbf{c},t)$. This function is a probably density such that $f(\mathbf{r},\mathbf{c},t)d\mathbf{r}\,d\mathbf{c}$ gives the number of electrons at positions $\mathbf{r}$ to $\mathbf{r}+d\mathbf{r}$ with velocities in the ranges $\mathbf{c}$ to $\mathbf{c}+d\mathbf{c}$ at time t. All the necessary information about the swarm can be obtained once $f(\mathbf{r},\mathbf{c},t)$ is known. Integration of $f(\mathbf{r},\mathbf{c},t)$ over all velocities gives the number density of electrons, $n(\mathbf{r},\mathbf{t})$.

Here we solve Eq. (1) by making the expansions

$$f(\mathbf{r},\mathbf{c},t)=\overline{w}(\alpha,c)\sum_{l=0}^{\infty}\sum_{m=-l}^{1}\sum_{\nu=0}^{\infty}\sum_{s=0}^{2}\sum_{\lambda=0}^{s}\sum_{\mu=-\lambda}^{\lambda}\times F(\nu lm|s\lambda\mu)R_{\nu l}(\alpha c)Y_m^{[l]}(\hat{\mathbf{c}})G_{\mu}^{(s\lambda)}n(\mathbf{r},t), \tag{2}$$

where $Y_m^{[l]}(\hat{\mathbf{c}})$ is a spherical harmonic, a function of the angles $\hat{\mathbf{c}}=\varphi,\phi$, $G_{\mu}^{(s\lambda)}$ denotes the sth application of gradient operator in irreducible tensor notation, $\overline{w}(\alpha,c)=(\alpha^2/2\pi)^{3/2}\exp(-\alpha^2c^2/2)$, is a Maxwellian distribution, $\alpha^2=m/kT_b$; T_b is a temperature parameter, $R_{\nu l}(\alpha c)=N_{\nu l}(\alpha c/\sqrt{2})^1S_{1+1/2}^{(\nu)}(\alpha^2c^2/2)$, $S_{1+1/2}^{(\nu)}(\alpha^2c^2/2)$ is a Sonine polynomial, $N_{\nu l}=\sqrt{2\pi^{3/2}\nu!/\Gamma(\nu+l+3/2)}$.

Substitution of expansion (2) into Eq. (1) and carrying out the necessary operations [1] and [2] reduces the Boltzmann equation to a set of matrix equation for the expansion coefficients $F(\nu lm|s\lambda\mu)$,

$$\sum_{l'}\sum_{m'}\sum_{\nu'}[M_{lm\nu,l'm'\nu'}+R\delta_{\nu'\nu}\delta_{l'l}\delta_{m'm}]\times F(\nu'l'm'|s\lambda\mu)=X_{lm\nu}(s\lambda\mu),$$

$$\nu,l=1,2,\ldots\infty;\quad m=-l,\ldots,+l. \tag{3}$$

Explicit expressions for the matrix of coefficients, $M_{lm\nu,l'm'\nu'}$, which contains the applied fields and collision dependence of the problem, and right hand side, $X_{lm\nu}(s\lambda\mu)$, are given in Ref. [2]. We note here that the expansion coefficients or ''moments'' are numbers that depend on the fields, the neutral number density n_0, and the collision cross sections. All the space-time and velocity dependence has been ''taken out'' by the above expansion of the phase-space distribution function. The velocity dependence of the moments is carried by the three indices l,m,ν, while the space dependence is carried by the three indices s,λ,μ. The spatial indices determine the order of the equation; $s=0$ is the spatially homogeneous equation, $s=1$ are the first order equations in ∇n, while $s=2$ are the second order equations in ∇n. The lowest order equation, $s=\lambda=\mu=0$, is an eigenvalue problem for the reaction rate R. For each value of (s,λ,μ) we have *one* matrix equation in the velocity indices (l,m,ν) to solve. Defining **E** to be in the z direction and **B** to be in the y direction, the transport coefficients expressed in terms of the moments are given by

$$R=-n_0\sum_{\nu=0}^{\infty}J_{0\nu}^0F(\nu00|000)=\text{rate coefficient}, \tag{4a}$$

$$W_x=-i\frac{\sqrt{2}}{\alpha}F(011|000)+in_0\sum_{\nu=0}^{\infty}J_{0\nu}^0F(\nu00|111)=\text{drift speed in the }\mathbf{E}\times\mathbf{B}\text{ direction}, \tag{4b}$$

$$W_z=\frac{i}{\alpha}F(001|000)-in_0\sum_{\nu=0}^{\infty}J_{0\nu}^0F(\nu00|110)=\text{drift speed in the }\mathbf{E}\text{ direction}, \tag{4c}$$

$$D_x=-\frac{1}{\alpha}[F(011|111)-F(01-1|111)]-n_0\sum_{\nu}J_{0\nu}^0\left[\frac{F(\nu00|200)}{\sqrt{3}}+\frac{F(\nu00|220)}{\sqrt{6}}-F(\nu00|222)\right]=\text{diffusion coefficient in the }\mathbf{E}\times\mathbf{B}\text{ direction}, \tag{4d}$$

$$D_y=-\frac{1}{\alpha}[F(011|111)+F(01-1|111)]-n_0\sum_{\nu}J_{0\nu}^0\left[\frac{F(\nu00|200)}{\sqrt{3}}+\frac{F(\nu00|220)}{\sqrt{6}}+F(\nu00|222)\right]=\text{diffusion coefficient parallel to the }\mathbf{B}\text{ field}, \tag{4e}$$

$$D_z=-\frac{1}{\alpha}F(010|110)-\frac{n_0}{\sqrt{3}}\sum_{\nu}J_{0\nu}^0\times[F(\nu00|200)+F(\nu00|220)]=\text{diffusion coefficient parallel to the }\mathbf{E}\text{ field}, \tag{4f}$$

$$D_h=-\frac{\sqrt{2}}{\alpha}[F(011|110)+F(010|111)]-n_0\sum_{\nu}J_{0\nu}^0F(\nu00|221)=\text{off-diagonal diffusion coefficient}. \tag{4g}$$

The drift velocity may also be expressed in terms of the drift speed W and the Lorentz or magnetic deflection angle ψ. That is,

$$W=\sqrt{W_x^2+W_z^2},$$

$$\tan(\Psi) = W_x / W_z .$$

To second order in $\nabla n (s=2)$, Eq. (3) gives
$s=0$,

$$\sum_{l'} \sum_{m'} \sum_{\nu'} [M_{lm\nu,l'm'\nu'} + R\delta_{\nu'\nu}\delta_{l'l}\delta_{m'm}] F(l'm'\nu'|000) = X_{lm\nu}(000), \quad (5a)$$

$s=1$,

$$\sum_{l'} \sum_{m'} \sum_{\nu'} [M_{lm\nu,l'm'\nu'} + R\delta_{\nu'\nu}\delta_{l'l}\delta_{m'm}] F(l'm'\nu'|11\mu) = X_{lm\nu}(11\mu), \quad \mu = -1,0,1, \quad (5b)$$

$s=2$,

$$\sum_{l'} \sum_{m'} \sum_{\nu'} [M_{lm\nu,l'm'\nu'} + R\delta_{\nu'\nu}\delta_{l'l}\delta_{m'm}] F(l'm'\nu'|200) = X_{lm\nu}(200), \quad (5c)$$

$$\sum_{l'} \sum_{m'} \sum_{\nu'} [M_{lm\nu,l'm'\nu'} + R\delta_{\nu'\nu}\delta_{l'l}\delta_{m'm}] F(l'm\nu'|22\mu) = X_{lm\nu}(22\mu), \quad \mu = -2,-1,0,1,2. \quad (5d)$$

For perpendicular fields we have the condition [2]:

$$F(l-m\nu|s\lambda-\mu) = (-1)^{m+\mu} F(lm\nu|s\lambda\mu).$$

Thus to second order in spatial gradients we have seven matrix equations to solve for, in order to determine transport up to diffusion. In the absence of reactions $J^0_{0v}=0$ and the summation terms in the above expressions for the transport coefficients vanish. This in turn implies that we only require the $s=0$ and $s=1$ expansion coefficients in order to determine transport processes up to diffusion. That is, in the absence of reactions we only require the solution of three equations to determine drift and diffusion. The coefficients as defined by Eq. (4) are the bulk transport coefficients [6]. The terms on the right hand side not included in the summation over the ν index give the flux component to the transport coefficient, while the summation term in the ν index represents the explicit effect of reactions on the transport coefficient due to the spatially nonuniform creation/annihilation of electrons. In the present investigation we only report the bulk transport coefficients. Investigation and discussion of flux and reactive contributions to transport in the presence of $\mathbf{E}\times\mathbf{B}$ fields will be left to later work.

For practical solution the expansions in the velocity space indices (l,m,ν) must be truncated. In the present work these three indices are truncated independently at $l_{\max}$, $m_{\max}$ ($\leqslant l_{\max}$), and $v_{\max}$ [2]. No upper limit is fixed on the ν or the l the indices and all three are incremented until the desired convergence is achieved. Thus the present approach is a true multiterm solution.

When a magnetic field is present it is often convenient to break up the transport into three regions, depending upon the relative strength of the magnetic field and the collision processes [2]. If we define

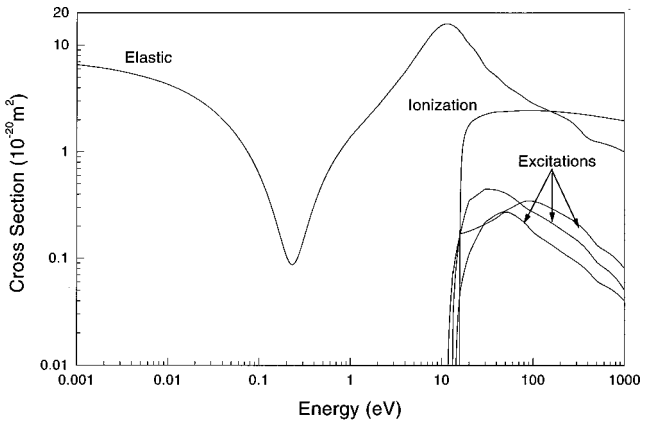

FIG. 1. The electron-argon cross section set of Biagi [4]. The three excitation processes have threshold energies of 11.55, 13.0, and 14.0 eV. The single ionization process has a threshold of 15.7 eV.

$$\Omega = \frac{e}{m} B$$

to be the electron cyclotron frequency and $\overline{\nu}$ to be some average collision frequency, then we have:
the weak magnetic field region

$$\Omega \ll \overline{\nu},$$

a moderate or intermediate magnetic field region

$$\Omega \sim \overline{\nu},$$

and the strong magnetic field region

$$\Omega \gg \overline{\nu}.$$

III. RESULTS AND DISCUSSION

For the argon cross sections we use the set of Biagi [7], which are shown in Fig. 1. This set of cross sections consists of the elastic cross section, one ionization process with a threshold of 15.7 eV, and three excitation processes with thresholds at 11.55, 13.0, and 14.0 eV. All scattering is assumed isotropic; this is a limitation of the set of cross sections, not the theory. Under the assumption of isotropic scattering, the elastic cross section is the same as the elastic momentum transfer cross section. A neutral temperature of 293 K is assumed and superelastic collisions are allowed for. For the ionization process we have randomly divided the available energy after ionization between the two post-ionization electrons [8]; we comment on this later. From Fig. 1 we expect two main features of the cross sections to dominate the electron transport: the deep minimum in the elastic cross section and the relatively closely spaced set of high threshold inelastic processes.

Figure 2 shows the mean electron energy as a function of E/n_0 from 0.001 to 5000 Td over a wide range of B/n_0 values from 0 to 50 000 Hx. The unit of a ''Townsend'' (Td) is well known in swarm physics [9]. The unit of a ''Huxley'' (Hx) is somewhat newer [2,10]. One Huxley is defined to be 10^{-27} T m^3. At a gas temperature of 293 K, one gauss per torr is equivalent to 3.034 Hx [11]. Thus for a gas pressure of

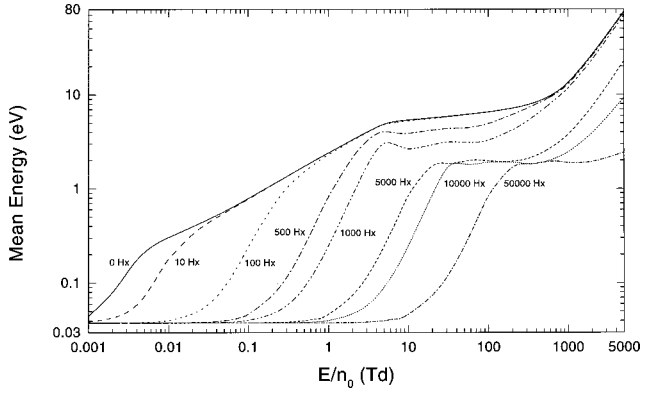

FIG. 2. Mean swarm energy as a function E/n_0 for a range of B/n_0 values, as indicated on the graph, for electrons in argon at $T_0=293$ K.

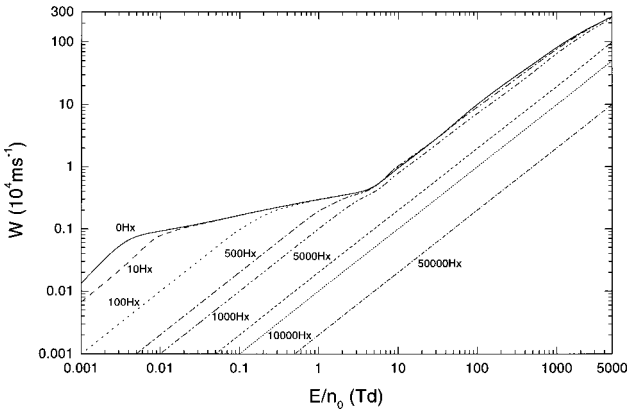

FIG. 4. Drift speed for electrons in argon for the same conditions as in Fig. 2.

one torr a B/n_0 value of 50 000 Hx corresponds to a magnetic field strength of approximately 16 500 G (1.65 T), a very strong magnetic field indeed.

From Fig. 2 we see four distinct regions of transport as E/n_0 increases. First, there is an initial plateau region where the electron energy is thermal $(3kT_0/2\sim 0.04\,\mathrm{eV})$. Second, there is a region of rapid rise due to the deep Ramsaur minimum. Third, there is a second plateau region brought about by the rapidly rising elastic cross section and the large energy loss of the electrons as the inelastic channels become important. This third region is the most interesting as far as transport phenomena are concerned as the transport coefficients contain structures that reflect the effect of the inelastic processes. Finally, there is another region of rapid rise, as both the elastic and inelastic processes drop off with high energy, and the electrons start to rapidly gain energy from the strong electric field. Note that in Fig. 2 as B/n_0 increases the mean energy curves move to the right. In particular the E/n_0 range of the thermal region increases with B/n_0, this is due to the reduction in electron heating caused by the perpendicular magnetic field [1,2]. Since, in general, the application of a magnetic field perpendicular to an electric field decreases the swarm mean energy one may view this as a ''cooling effect.'' Note also that for the higher values of B/n_0, the mean energy shows a region of decrease with increasing E/n_0! This behavior is more evident for the intermediate values of B/n_0, see, for example, the $B/n_0=1000$-Hx curve in the 4-Td region, and is contrary to previous experiences in swarm physics. One would expect the mean swarm energy to increase with increasing E/n_0. This is discussed in detail below.

Figure 3 shows the ionization rate coefficient R/n_0 for the same range of values of E/n_0 and B/n_0 as the mean energy. These curves are basically featureless as ionization only becomes significant at the higher values of E/n_0 when sufficient electrons have enough energy to undergo ionization. The curves show the expected increase in R/n_0 with E/n_0 and decrease in R/n_0 with B/n_0. In Figs. 4 and 5 the drift speed and the tangent of the Lorentz angle are shown. From Fig. 4 we observe that the drift speed shows little sensitivity to the details of the cross sections, even for weak B/n_0. In the limit of large B, $W=E/B$ and the curves in Fig. 4 become straight lines of slope 1. For these values of B/n_0 the strong magnetic field dominates the collisions $(\Omega\gg\nu)$ for the entire range of E/n_0 and this transport coefficient reflects little of the energy dependence of the cross sections. For the weak values of B/n_0 some sensitivity to the cross sections is evident; primarily to the steeply rising elastic cross section where the rate of increase of W with E/n_0 drops off. On the other hand, Fig. 5 shows that $\tan(\psi)$ is sensitivity to the scattering cross sections even for large values of B/n_0. The

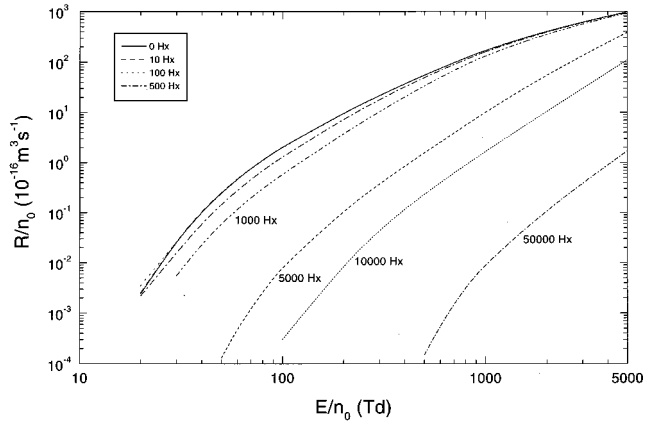

FIG. 3. Ionization rate coefficient for electrons in argon at $T_0=293$ K as a function of E/n_0 for the same range of B/n_0 values as in Fig. 2.

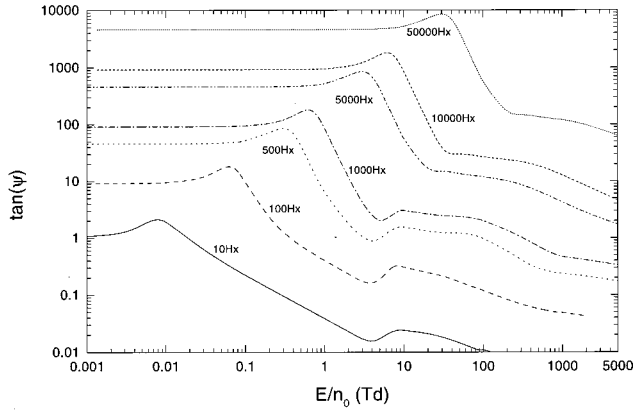

FIG. 5. Tangent of the Lorentz for electrons in argon for the same conditions as in Fig. 2.

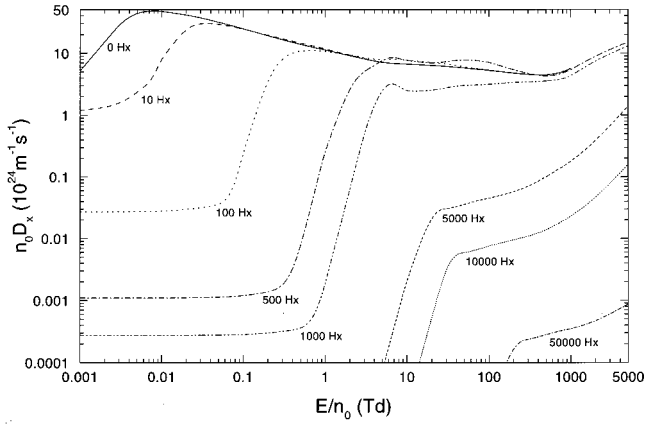

FIG. 6. The diffusion coefficient in the $\mathbf{E}\times\mathbf{B}$ direction for electrons in argon for the same conditions as in Fig. 2.

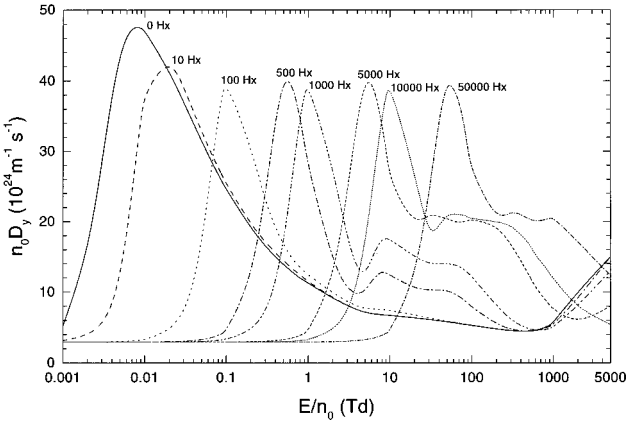

FIG. 8. The diffusion coefficient in the $\mathbf{B}$ direction for electrons in argon for the same conditions as in Fig. 2.

sensitivity of $\tan(\psi)$ to the cross sections has been discussed by Schmidt [10]. Consider a large value of B/n_0, for weak E/n_0 the mean energy is essentially thermal and the magnetic field dominates the transport. Thus $\tan(\psi)$ is very large, indicating that all the drift is essentially $\mathbf{E}\times\mathbf{B}$. As E/n_0 increases the mean energy increases and $\tan(\psi)$ also increases as the elastic cross section drops and the dominance of the B field increases. Thus the maximum in $\tan(\psi)$ reflects the minimum in the elastic cross section. Now as E/n_0 increases further the mean energy passes through the minimum in the elastic cross section and the electrons encounter a rapidly rising cross section. This reduces the dominance of the B field and $\tan(\psi)$ starts to drop steeply. However, as E/n_0 increases further, inelastic scattering becomes significant, feeding low energy electron into the swarm. This leads to a plateauing out of the increase in mean energy with E/n_0 and the rate of decrease of $\tan(\psi)$ with E/n_0 drops in response. Note that for the moderate to weak values of B/n_0 we start to see some structure in $\tan(\psi)$ after the rapid drop, this is most likely due to the inelastic processes.

The diagonal diffusion coefficients D_x, D_z, and D_y are shown in Figs. 6, 7, and 8. All these coefficients reflect to some degree the four regions of transport. At first sight the two diffusion coefficients perpendicular to the magnetic field, D_x (diffusion along the $\mathbf{E}\times\mathbf{B}$ direction) and D_z (diffusion along the $\mathbf{E}$ direction) show similar behavior with E/n_0,

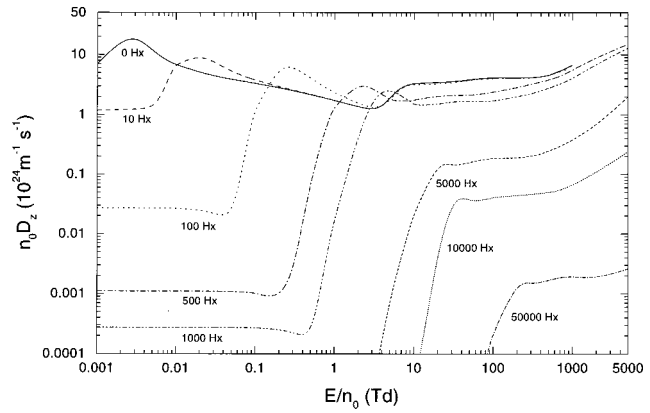

FIG. 7. The diffusion coefficient in the $\mathbf{E}$ direction for electrons in argon for the same conditions as in Fig. 2.

particularly at the higher B/n_0 values. The rapid rise in both D_x and D_z is a consequence of the deep Ramsaur minimum at approximately 0.2 eV (see Fig. 1). Note that as B/n_0 increases both D_x and D_z in general decrease markedly. In fact, both coefficients may vary over several orders of magnitude with both B/n_0 and E/n_0. This is a consequence of a dominant magnetic field reducing diffusion perpendicular to itself by holding the electrons in orbits. Again we note that for these coefficients the intermediate values of B/n_0 reveal more structure after the rapid rise than either the low or high values of B/n_0; indicating a heightened sensitivity to the inelastic processes. In the thermal limit (weak E/n_0), both n_0D_x and n_0D_z decrease as $(B/n_0)^{-2}$ [12].

The diffusion coefficient parallel to the magnetic field, D_y, shown in Fig. 8 stands in contrast to both D_x and D_z. The variation in D_y with both B/n_0 and E/n_0 is relatively very small when compared to that for diffusion perpendicular to the magnetic field. The reasons for this have been given in earlier work [2]. Unlike D_x and D_z, the magnetic field has no explicit effect upon D_y. Like $\tan(\psi)$, D_y shows a high sensitive to the energy dependence of the cross sections. This coefficient clearly shows the four regions that dominate the transport. The initial flat part of the curves at low values of E/n_0 where D_y is effectively constant corresponds to the thermal region. In this region D_y is essentially the thermal diffusion coefficient and unlike D_x and D_z the value of D_y does not decrease with increasing B/n_0, the thermal value of D_y does of course extend over a larger range of E/n_0 values as B/n_0 increases. The maximum in D_y reflects the Ramsaur minimum, where due to the rapidly falling collision frequency the diffusion is substantially enhanced. After the maximum in diffusion we enter the third region where there is an initial sharp drop in D_y due to the rapidly rising elastic cross section. Here the inelastic collisions start to exert their influence on the swarm. Their direct effect is to enhance collisions and thereby reduce diffusion. However, due to the large threshold energies involved in these processes, at certain values of E/n_0 they scatter electrons back in energy to the minimum region of the elastic cross section and this will tend to enhance diffusion. Thus we have a secondary maximum and plateau region in D_y which breaks up the drop off. Like the mean energy, the secondary maximum is more pronounced for the intermedi-

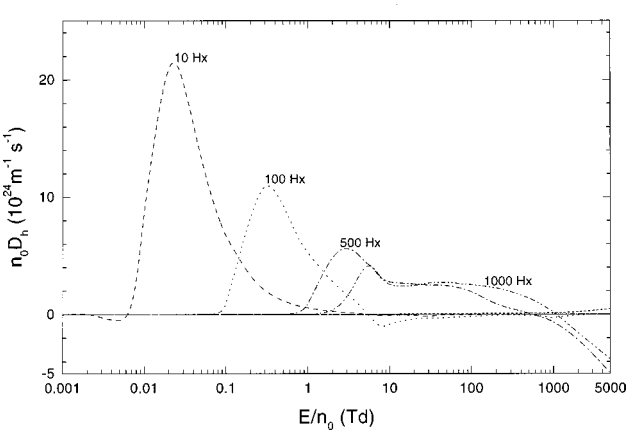

FIG. 9. The off-diagonal diffusion coefficient for electrons in argon for the same conditions as in Fig. 2.

ate values of B/n_0. Beyond this the drop off in D_y continues until all cross sections fall off and D_y rises again (this is the fourth region of transport).

For the sake of completeness, the off-diagonal diffusion coefficient is shown in Fig. 9. This coefficient may be either positive or negative [2], hence Fig. 9 is a log-linear plot. On the scale shown, the higher B/n_0 values of D_h (5000, 10 000, and 50 000 Hx) are too small to be shown.

As noted above, perhaps the most interesting region of transport is region three, i.e., those field combinations for which the swarm mean energy corresponding in energy to the region in the cross sections where the elastic cross section is rapidly rising and the inelastic processes become significant. In Fig. 10 the mean electron energy for $B/n_0 = 1000$ Hx is shown as a function of E/n_0 in the range 1–150 Td. On this scale, Fig. 10 (the solid curve) clearly shows a region of decreasing mean energy with increasing E/n_0, in fact the curve has two maximums. In the E/n_0 region of the two maximums the convergence accuracy in the mean energy is better than 1%, while the variation in the mean energy over the same region is approximately 15%. Referring back to Fig. 2 it is important to note that this phenomenon does not occur for zero or weak magnetic field, the presence

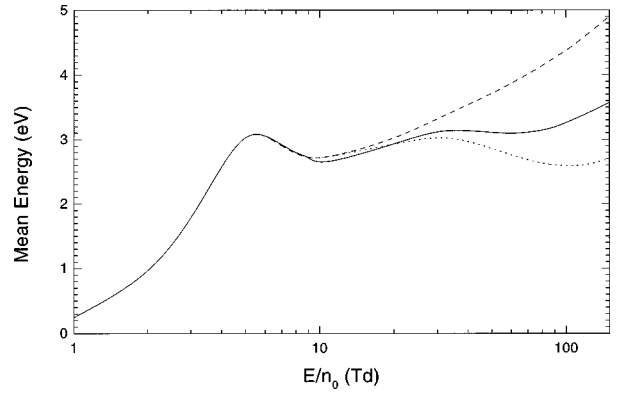

FIG. 10. The mean swarm energy for electrons in argon at $T_0 = 293$ K as a function of E/n_0 for $B/n_0 = 1000$ Hx. (solid curve) The long-dashed curve gives the mean energy when the ionization process is reduced to an inelastic collision—see text. The short-dashed curve gives the mean energy when the available energy after an ionizing collision is partitioned in the fixed ratio 1:0.

of a comparatively strong magnetic field is essential, however, too strong a magnetic field tends to reduce the effect. The phenomenon is due to the combined effect of ''magnetic field cooling'' and ''inelastic/ionization cooling.''

The cooling effect of applying a magnetic field perpendicular to the electric field is well known and has been discussed in earlier work [2,12,13]. In the present work we will refer to this as ''magnetic field cooling'' for the sake of conciseness. The term ''inelastic cooling'' simply refers to the fact that whenever an electron under goes an inelastic collision it losses at least the threshold energy of the excitation process and emerges from the collision with reduced energy. If the electron has energy just above the threshold energy, then in any inelastic encounter with a neutral it will lose almost all its energy, resulting in a substantial cooling effect on the swarm, even if only a relatively small fraction of the electrons have the required energy. We now introduce a third term to be used in the discussion below: ''ionization cooling.'' This term was used earlier by Robson and Ness [14]. Ionization cooling is essentially the same as inelastic cooling with the additional cooling effect of the dilution of the swarm energy due the creation of the new electrons. That is, following an ionization collision, the remaining energy available after the collision is shared between two electrons, instead of only one, further reducing the mean energy. If the motion of the neutrals is ignored then, after an ionizing collision, of threshold energy ε_i, between an electron of kinetic energy ε and a neutral, there will be an amount of energy $\varepsilon - \varepsilon_i$ available to be shared between the two post collision electrons. The way this available energy is partitioned between the two post collision electrons will effect the transport coefficients particularly as the ionization rate becomes significant. This has been demonstrated in the **E** only situation [8]. In the current investigation, in the absence of more precise knowledge we have randomly divided the available energy $\varepsilon - \varepsilon_i$ between the post collision electrons. Thus, if after an ionizing collision one of the electrons acquires a fraction $\Delta (0 \leqslant \Delta \leqslant 1)$ of the available energy, the other electron must acquire the fraction $1 - \Delta$. So far in the current investigation, all fractions Δ are equiprobable.

Returning now to Fig. 10, between 1 and 5 Td, the mean swarm energy increases from approximately 0.25 to 3 eV. Note that from Fig. 2, for zero magnetic field the mean energy over the same range of E/n_0 is substantially higher. Now at $E/n_0 \sim 5$ Td with $\overline{\varepsilon} \sim 3$ eV an increasing number of electrons in the tail of the energy distribution function have sufficient energy to undergo the high threshold inelastic processes and thus inelastic cooling occurs. As E/n_0 is increased further more electrons in the tail undergo inelastic scattering and inelastic cooling is enhanced. The combined effect of magnetic field cooling and inelastic cooling actually decreases the swarm mean energy as E/n_0 increases from about 6 to 10 Td. From 10 to about 35 Td the mean energy increases with E/n_0 as the energy input from the electric field overcomes both magnetic field cooling and inelastic cooling. At approximately 35 Td we observe a second maximum in $\overline{\varepsilon}$ followed by a subsequent decrease until about 60 Td. This second decrease in $\overline{\varepsilon}$ with E/n_0 is a consequence of the combined effect of magnetic field cooling and the dilution effect of ionization cooling. Referring to Fig. 3, we see that the ionization rate coefficient becomes significant at

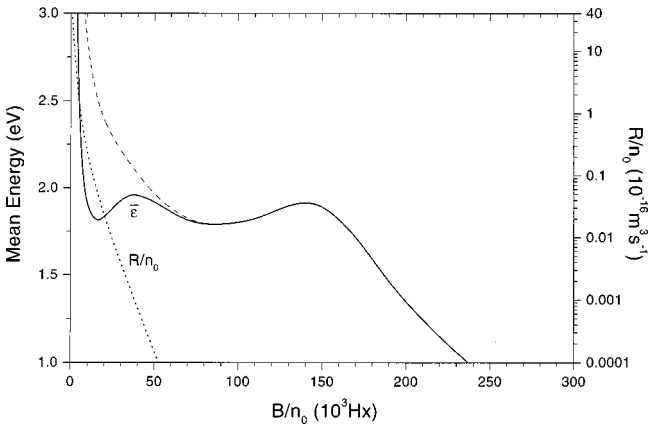

FIG. 11. The mean swarm energy for electrons in argon at $T_0 = 293$ K as a function of B/n_0 for $E/n_0 = 500$ Td (solid curve). The long-dashed curve gives the mean energy when the ionization process is reduced to an inelastic collision. The short-dashed curve is the ionization rate coefficient as a function of B/n_0 for $E/n_0 = 500$ Td.

around 30 Td. The long-dashed curve in Fig. 10 is the mean energy calculated by treating ionization as just another inelastic process, i.e., no secondary electrons are produced. This was done by setting the term in the ionization collision operator that models the generation of the new electron to zero and resolving the Boltzmann equation. When this is done the second maximum in $\overline{\varepsilon}$ disappears, as there is no longer any ionization cooling. The third curve in Fig. 10, the short-dashed curve, gives the mean swarm energy when Δ is set to 1. That is, one of the post ionization electrons gets all the energy while the other gets none. This is perhaps the most ''extreme'' partitioning scheme. Again we observe the second peak, but there is no effect upon the first peak, further supporting our hypothesis that the first peak is due the combined effects of magnetic field and inelastic cooling, while the second peak is due to the combined effect of magnetic field cooling and the dilution effect of ionization cooling. In this case the effect of ionization cooling is enhanced, as the second maximum occurs with a lower mean energy and the subsequent decrease in the mean energy is greater and extends over a larger range of E/n_0.

The combination of magnetic field and inelastic/ionization cooling leads to another interesting phenomenon at very high B/n_0 for strong electric fields. Figure 11 (solid curve) shows the mean swarm energy at $E/n_0 = 500$ Td as a function of B/n_0 from 0 to 300 000 Hx. As stated above, the application of a magnetic field perpendicular to an electric field will tend to cool a swarm. Previously it was predicted that for a fixed E/n_0, $\overline{\varepsilon}$ would always decrease with B/n_0, independent of the cross sections [1]. Figure 11 shows that this is not the case. From Fig. 11 we see that there are two maximums in $\overline{\varepsilon}$, at approximately 35 000 and 140 000 Hx. In the B/n_0 region of the two maximums the convergence accuracy for the mean energy is better than 0.5%, while the variation in the mean energy over the same region is approximately 10%. From 0 to 10 000 Hx $\overline{\varepsilon}$ decreases sharply with B/n_0 as magnetic field cooling and ionization/inelastic cooling combine to rapidly cool the swarm. By 10 000 Hx the mean energy has fallen to below 2 eV. However, as the swarm rapidly cools, the ionization rate R/n_0, shown by the short-dashed curve in Fig. 11, rapidly falls. The more energetic electrons, the ones in the high-energy tail, are the electrons undergoing ionizing/inelastic collisions and thus cause ionization/inelastic cooling. However, they are also the electrons most influenced by magnetic field cooling. As the swarm cools with increasing B/n_0, the tail population drops sharply and so does the ionization and inelastic collision rates, as they now compete with magnetic field cooling. In response the rate of cooling of the swarm slows. At high enough B/n_0 ionization all but shuts down and the heating effect of the strong electric field overcomes the magnetic field cooling and the diminished inelastic cooling for a range of increasing B/n_0 values (approximately 15 000–40 000 Hx). This produces the first peak. After this $\overline{\varepsilon}$ decreases with B/n_0 once more until inelastic cooling shuts down. This shutdown of inelastic cooling produces the second maximum at around 140 000 Hx. After the second peak the cooling is essentially magnetic field cooling only and $\overline{\varepsilon}$ drops of as B^{-2}, the expected strong B-field limit [12]. As in Fig. 10, the long-dashed curve in Fig. 11 is the mean energy calculated by treating ionization as an inelastic process only. Note that this curve only has the higher B/n_0 maximum, i.e., there is no peak associated with the shutdown of the dilution effect of ionization cooling.

In general convergence of the present solution in all three indices and for all coefficients was good, better than 0.1%. However, for strong electric field, convergence in the ν index deteriorated, particularly for low values of B/n_0. The diffusion coefficients were the first to exhibit convergence difficulties. For the low values of B/n_0 convergence in the ν index for the diffusion coefficients rapidly deteriorated ($>10\%$) above 1000 Td. Above 5000 Td, for the low values of B/n_0, convergence of all coefficients was unsatisfactory. For the higher values of B/n_0 the rapid deterioration in convergence of the diffusion coefficients occurred above 5000 Td. Note that from Fig. 2 this region of deteriorating convergence corresponds to region 4 of transport, i.e., the second region in E/n_0 of rapid energy rise. Some what less serious convergence difficulties in the ν index were also encountered at the beginning of region 3 of transport (corresponding to the start of the second plateau region in energy in Fig. 2) for the intermediate values of B/n_0. For example, for $B/n_0 = 1000$ Hx in the region between 5 and 20 Td convergence in $\overline{\varepsilon}$, W_x, W_z, and D_y was better than 1%, while convergence in D_x, D_z, and D_h was within 5%.

IV. CONCLUSION

A comprehensive investigation of electron transport in argon in the presence of crossed electric and magnetic fields has been carried out. The mean energy, the ionization rate, the drift velocity and the diffusion tensor have been calculated over a wide range of E/n_0 and B/n_0 values. This study was initiated in order to obtain transport data for input into a fluid model of an argon magnetron discharge [15] and has resulted in a database of such transport data. In the course of the investigation a number of issues of fundamental interest arose.

First, the sensitivity of both the Lorentz angle and the diffusion coefficient along the magnetic field to the energy

dependence of collision cross sections was noted. Again highlighting the potential use of $\mathbf{E}\times\mathbf{B}$ transport data in the determination of low-energy electron-neutral scattering cross sections [10]. The variation of the mean energy and the transport coefficients with E/n_0 depends upon both the energy dependence of the collision cross sections and the value of B/n_0. In general this variation shows a greater sensitivity to the energy dependence of the cross sections for intermediate values of B/n_0 where $\Omega \sim \overline{\nu}$. For weak values of the magnetic field where $\Omega \ll \overline{\nu}$, the collisions are too dominate and the influence of the magnetic field is diminished. On the other hand, for strong magnetic fields where $\Omega \gg \overline{\nu}$, the magnetic field is too dominate and the sensitivity to the cross sections is diminished.

Second, contrary to previous experience in swarm physics, we find regions were the mean-swarm energy decreases with increasing electric field and increases with increasing magnetic field. These phenomena were associated with the interplay between magnetic field cooling and inelastic/ionization cooling, although the role of the cross sections in both phenomena is of course vital. This is the subject of current investigation and a number of highly idealized model interactions have been investigated; these will be reported at a later date. At this stage it appears that two ingredients are essential. First, there must be a high threshold inelastic/ionization process with the threshold well above thermal energy. Second, the elastic cross section requires a region where it increases sharply with energy. Argon satisfies both these conditions. In comparison to the normally good convergence, some decrease in convergence accuracy was encountered in the region of these phenomena. However, the variation in the mean energy due to these phenomena was over an order of magnitude greater than the convergence accuracy in the mean energy in these regions. The decrease in convergence possibly reflects some ''extreme'' form of the energy distribution in these regions. Nevertheless, it would be useful to the have the present finding verified by an independent study, such as a Monte Carlo simulation investigation.

ACKNOWLEDGMENTS

This work was supported by the Monbusho International Scientific Program, Grant No. 08044169. The authors would also like to thank Dr. R. W. White for interesting discussions and helpful comments.

[1] K. F. Ness, Phys. Rev. E **47**, 327 (1993).
[2] K. F. Ness, J. Phys. D **27**, 1848 (1994).
[3] T. Makabe, *Plasma Electronics* (in Japanese) (Bifukan, Tokyo, 1999).
[4] A. Itoh, T. Makabe, N. Shimura, and S. Tougo, IEEE Trans. Plasma Sci. **24**, 109 (1996).
[5] M. A. Lieberman and A. J. Lichtenberg, *Principles of Plasma Discharges and Materials Processing* (Wiley, New York, 1994).
[6] R. E. Robson, Aust. J. Phys. **44**, 685 (1991).
[7] S. F. Biagi (private comminication).
[8] K. F. Ness and R. E. Robson, Phys. Rev. A **34**, 2185 (1986).
[9] L. G. H. Huxley and R. W. Crompton, *The Diffusion and Drift of Electrons in Gases* (Wiley, New York, 1974).
[10] B. Schmidt, Comments At. Mol. Phys. **28**, 379–95 (1993).
[11] This is the same conversion factor (3.034) between the Townsend (10^{-21} V m^2) and E/p expressed in V/cm/torr. See Ref. [8] above.
[12] K. F. Ness and R. E. Robson, Phys. Scr. **T53**, 5 (1994).
[13] K. F. Ness, Aust. J. Phys. **48**, 557 (1995).
[14] R. E. Robson and K. F. Ness, J. Chem. Phys. **89**, 4815 (1988).
[15] E. Shidoji, K. F. Ness, and T. Makabe, Vacuum (to be published).